



25<sup>th</sup> ABCM International Congress of Mechanical Engineering  
October 20-25, 2019, Uberlândia, MG, Brazil

## LAP TIME SIMULATIONS SUPPORTED BY EXPERIMENTAL DATA

**Adriano Schommer**

**Jonny Carlos da Silva**

Department of Mechanical Engineering, Federal University of Santa Catarina, Florianópolis, Brazil  
adriano.schommer@gmail.com, jonny.silva@ufsc.br

**Rodrigo de Souza Vieira**

Department of Mechanical Engineering, Federal University of Santa Catarina, Florianópolis, Brazil  
rodrigo.vieira@ufsc.br

**Abstract.** *This work focuses on lap time simulations to deal with the introduction of a new circuit in a racing car competition. Due to the limited running costs of an entry-level racing team, tests and measurement of vehicle parameters are restrict, which limits the use of complex simulations. To deal with this issue, experimental data from previously race events supported the estimation of parameters. In this work, Monte Carlo method was used to estimate drag coefficient, drivetrain efficiency and tire/road coefficient of friction. Two sets of data were acquired for this work: training data, from Ayrton Senna Circuit - GO, used to estimate the parameters, and Cristais Circuit – MG, used to validate the vehicle model.*

**Keywords:** *Data acquisition, motorsport, racecar, lap time simulation.*

### 1. INTRODUCTION

The context of this research relies on the Brazilian touring car championship *Brasileiro de Marcas*. Established in 2011, it promoted vehicle manufactures by racing silhouette racecars, resembling compact sedans such as: Toyota Corolla, Renault Fluence, Ford Focus and Chevrolet Cruze. In 2016, a new track, known as Cristais Circuit, in Minas Gerais state, was introduced to the race calendar. The problem addressed in this paper is related to the challenges derived from scarce data available to setup racecars for a new circuit, and the short time to prepare drivers during the race event.

Even though lap time simulation is a well-established engineering tool, it is rarely used by entry motorsport categories. Accurate vehicle models are complex, which involves many input parameters not easily measurable, and/or expensive simulation packages. However, when it comes to speed profile for circuit recognition, instead of detailed vehicle behavior, overall vehicle dynamics reduces the need of complexity of the vehicle model at cost of accuracy and lack of details to explore vehicle parameters.

The simplest model available is a single-point of mass with a constant coefficient of friction between tire and road. The application of such simple models to generate speed profile of a circuit has been referred in the literature (Segers, 2014; Rouelle, 2014). However, results from simulations and how consistent these models are for various circuits were not discussed. Furthermore, the usefulness of such data for circuit recognition, and a method to populate such models with logged data has not been addressed. In other words, could a small racing team benefit from lap time simulations? This is the main motivation for this work

### 2. MATERIALS AND METHODS

#### 2.1 Racecar and Data Acquisition

All vehicles of the *Brasileiro de Marcas* championship were front-wheel-drive powered by a four-cylinders naturally aspirated engine. A 2016 Toyota Corolla racecar was the source of experimental data for this research. The data acquisition system of the racecar consists into a MoTeC SDL3 dashboard, with 16 MB of logging memory and an integrated 3-axis accelerometer ( $\pm 5G$ ) logged at 25 Hz. The dashboard also records data from an analogue steering angle sensor (25 Hz) and a GPS MoTeC L10 connected via RS-232 serial port (10 Hz).

The 2016 season provided eight events that were held in seven different Brazilian circuits from which data were gathered. These vehicles were slightly modified from the previously years, with the most significant change being a lower limit for engine maximum speed. For this reason, only 2016 data were used in order to avoid diverged data on the parameter estimation process. Two sets of data were acquired for this work: training data, from Ayrton Senna Circuit - GO, used to estimate the parameters, and Cristais Circuit – MG, used to validate the vehicle model.

## 2.2 Vehicle model

The underlying concepts of the lap time simulations presented in this paper relies on the G-G diagram, a plot of longitudinal acceleration against lateral acceleration of a racecar, expressed as units of gravitational acceleration. In motor racing, it is a typical measure of the overall vehicle performance, combining driver, vehicle and road performances. As speed increases, cornering and braking ability are positively affected by aerodynamic forces, while forward acceleration is negatively affected by higher external resistances such aerodynamic and rolling resistances.

The velocity profile of the vehicle was simulated in this work based on the assumption of a point-mass being driven at the boundaries of the G-G diagram. The vehicle model consists of a point-mass reacting to external forces limited by its tire/road coefficient of friction ( $\mu$ ). This coefficient  $\mu$  is assumed to limit both, lateral ( $a_y$ ) and longitudinal ( $a_x$ ) car accelerations. Furthermore, in this work  $\mu$  is considered constant, leading to the following assumptions:

1. The grip available at the racetrack does not change.
2. The constant coefficient of friction acts as if the tire were operating at its optimum slip angle and slip ratios.
3. Any changes in tire load neglects changes of the friction coefficient.

Figure 1 summarizes the vehicle model assumptions by its performance envelope, defined here as a G-G diagram.

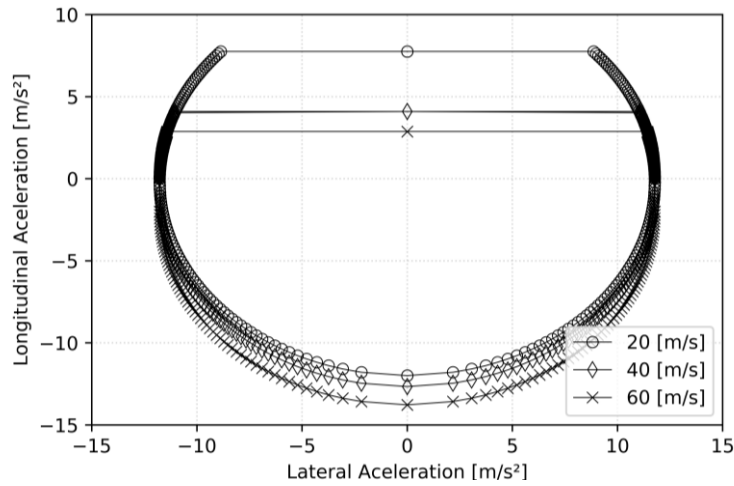


Figure 1: Modeled performance envelope of the vehicle as function of speed

In Fig. 1, the upper part of the G-G diagram is trimmed by engine power and gearbox ratio. At the bottom part, deceleration is improved due to the additional resistance forces. The effect of the coefficient of friction being constant is better seen on the sideways of the diagram, which is limited at the same lateral acceleration independent of the speed. In fact, it would change with speed, improving lateral acceleration at higher speeds due to the additional tire load provided by aerodynamic forces. Equation (1) expresses the assumed coefficient of friction ( $\mu$ ) as function of the vehicle maximum lateral acceleration.

$$\mu = \mu_y = \frac{F_y}{m \cdot g} = \frac{a_y}{g} \quad (1)$$

In this equation,  $\mu$  is the assumed coefficient of friction [-],  $\mu_y$  is the lateral coefficient of friction [-],  $F_y$  is the lateral force generated by the tires [N],  $m$  is the overall mass of the vehicle [Kg],  $a_y$  is the lateral acceleration [ $m/s^2$ ] and  $g$  is the gravitational acceleration [ $m/s^2$ ].

According to Segers (2014), although simple, a point-mass vehicle model is able to generate a velocity profile in a given circuit with satisfactory accuracy to draw conclusions about the characteristics of a circuit. In this research, vehicle model was implemented by the means of power flow in the multiport-domain Advanced Modeling Environment for Simulation (AMESim®) software. The main concept of such simulation environment lies on the power flow between components, given by the product of flow and effort variables (SILVA, 2005). Figure 2 shows the vehicle model concept:

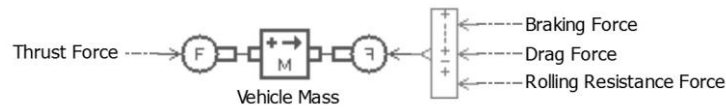


Figure 2: Vehicle model concept.

In this model, the equation of motion is defined as follows:

$$m \cdot a_x = F_e - (F_b + F_d + F_r) \quad (2)$$

Where,  $a_x$  is the forward acceleration [m/s<sup>2</sup>],  $F_e$  is the thrust force [N],  $F_b$  is the braking force [N],  $F_d$  is the drag force [N] and  $F_r$  is the rolling resistance force [N]. In the next sections, each of these forces is further explored.

### 2.3 Thrust force

For a low powered vehicle, most part of the time longitudinal acceleration is limited by the engine and not by the tires (SEGERS, 2014). Based on this statement, this work considers that wheel spin does not occur when throttle is applied. This assumption allows designing a driver controller in such manner that thrust force from engine is always present whenever forward acceleration is not limited by braking and/or trail braking on cornering maneuvers. In other words, the throttle either is off or applied at wide-open throttle (WOT). The thrust force ( $F_e$ ) is given by Eq. (3), and the model implementation of the powertrain is shown in Fig. 3.

$$F_e = \frac{T \cdot i_n}{R_R} \quad (3)$$

In Eq. (3),  $T$  is the engine torque [N.m],  $i_n$  is the gear ratio [-] and  $R_R$  is the effective rolling radius of the tire [m].

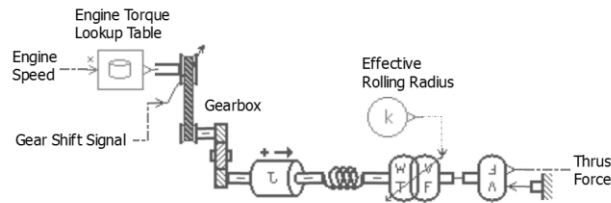


Figure 3: Powertrain model.

The powertrain model shown in Fig. 3 is also a product of manipulation of effort and flow variables, embedded in the equations of each component. However, instead of translational mechanics presented before, the power is given by rotational mechanics where the effort variable is a torque [N.m] and flow variable is an angular velocity [rad/s].

In this model, engine torque is taken from a lookup table as function of engine speed. This torque is multiplied by a gear ratio according to the engaged gear on the gearbox and is transmitted to the traction wheels as power from the driveline torque (effort variable) and the wheel angular speed (flow variable). Finally, thrust force is derived from the effective rolling radius of the tires.

From the powertrain model, thrust force is applied to the vehicle mass, as shown in Fig. 2. Inertia and rigidity of the drivetrain components are necessarily included to respect the causality between physical components in the multiport environment, although their values are considered negligible.

### 2.4 Braking force

According to the concept of tire friction circle, maximum braking force is achieved when braking in a straight line and must decrease as lateral force builds up (Milliken and Milliken, 1995). This phenomenon happens to accommodate the longitudinal and lateral forces to the available tire grip. In fact, grip is the total force available in the tires ( $F_t$ ) and is function of lateral force ( $F_y$ ) and braking force ( $F_b$ ) vectors. When braking force is maximum, lateral force is zero and vice versa. Maximum tire force is given by Eq. (4), lateral force by Eq. (5) and the relation between these three forces is presented by Eq. (6).

$$F_t = m \cdot g \cdot \mu \quad (4)$$

$$F_y = \frac{m \cdot v_c^2}{R} \quad (5)$$

$$F_t^2 = F_y^2 + F_b^2 \quad \therefore (m \cdot g \cdot \mu)^2 = \left(\frac{m \cdot v_c^2}{R}\right)^2 + F_b^2 \quad (6)$$

In the equations above,  $F_t$  is the total force available at the tires,  $F_y$  is the lateral force and  $F_b$  is the braking force,  $v_c$  is the maximum cornering velocity [m/s] and  $R$  is the cornering radius [m].

Isolating braking force ( $F_b$ ) from Eq. (6), Eq. (7) is given as function of lateral and total tire forces.

$$F_b = \sqrt{(m \cdot g \cdot \mu)^2 - \left(\frac{m \cdot v_c^2}{R}\right)^2} \quad (7)$$

In cornering maneuvers, lateral force starts to build up as braking force starts to decrease until it reaches zero at the apex of a corner. At this moment, only lateral force ( $F_{y@apex}$ ) is acting on the tires and it takes all available force ( $F_t$ ). Thus, the maximum speed that a vehicle could perform a given corner, in this paper called *maximum cornering velocity* ( $v_c$ ), can be isolated from Eq. (7) and defined by friction coefficient ( $\mu$ ), and the corner radius ( $R$ ) such as:

$$F_{y@apex} = F_t \quad \therefore \frac{m \cdot v_c^2}{R} = m \cdot g \cdot \mu \quad \xrightarrow{\text{yields}} \quad v_c = \sqrt{g \cdot \mu \cdot R} \quad (8)$$

Where,  $F_{y@apex}$  is the lateral force at corner apex.

## 2.5 External resistance forces

Drag force is the only aerodynamic effect acting on this point-mass vehicle model. It is a vector force on longitudinal axis in the negative direction (against thrust force) and its magnitude is calculated by the classic equation (KATZ, 1995):

$$F_d = \frac{1}{2} \cdot \rho \cdot C_d \cdot A \cdot v_x^2 \quad (9)$$

Where,  $\rho$  is the air density [kg/m<sup>3</sup>],  $C_d$  is the drag coefficient [-],  $A$  is the frontal area of the car [m<sup>2</sup>] and  $v_x$  is the forward velocity [m/s].

Rolling resistance was modeled according to Jazar (2008) Eq. (10) as function of a rolling resistance coefficient ( $u_r$ ), given by a second order polynomial Eq. (11), and the vertical force applied to tires. In this work, vertical force is the total vehicle weight and is kept constant over the time:

$$F_r = u_r \cdot m \cdot g \quad (10)$$

$$u_r = u_0 + u_1 \cdot v_x^2 \quad (11)$$

Where,  $u_0$  [-] and  $u_1$  [ $\frac{s^2}{m^2}$ ] are experimental coefficients to fit rolling resistance data. According to Jazar (2008), typical values are  $u_0 = 0.015$  and  $u_1 = 7e^{-6}$ . Although these values have been applied to passenger cars tires, they were used here due to the lack of parameters available for the racing tires used in the object of study of this work.

## 2.6 Circuit model

Because there was no previously logged data for the Cristais Circuit at the time this work was conducted, a different approach for circuit parameterization was taken with the help of a computer-aided design (CAD) software. Aiming to test the method, the parameterization of the known Ayrton Senna Circuit was first performed supported by previously GPS logged data. Circuit map and the driver racing line were overlaid with the help of the GPS coordinates of a flying lap at the circuit. This process resulted in a scaled image imported to a CAD software where the racing track could be broken down into a series of constant radius arcs and straight lines.

To simulate progressive steering increase towards corner apexes, corners are typically split into a series of decreasing arc radius (SIEGLER; DEAKIN; CROLLA, 2000). To reduce CAD modeling time, in this work the racing line was split into coarse sectors of constant radius instead of decreasing radius. Then, to simulate the progressive steering, with the help of Pandas library in Python the data was up-sampled 16 times by a linear interpolation and further smoothed by a

rolling mean function with a window size of 20 observations. The result of this process, called here as Rolling Mean Track Data, is compared with raw track data in Fig. 4.

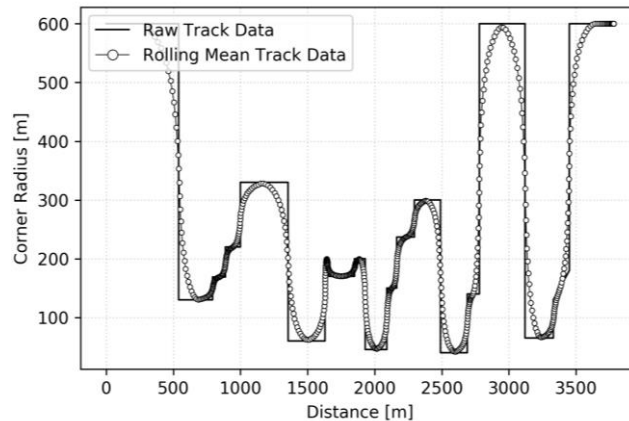


Figure 4: Rolling mean method of circuit parameterization.

Figure 4 shows the effects of the Rolling Mean Track Data method at the transitions between straight lines and corners, where progressive corner radius are achieved. Straight lines were modeled as a corner with 600m of radius, which was large enough to not limit forward acceleration due to the limit of adhesion. For the Cristais Circuit, the parameterization process was performed in a similar manner. However, due to the lack of GPS data, the racing line was drawn with the help of driver’s expertise.

### 3. PARAMETER ESTIMATION

#### 3.1 Design exploration

According to Witten, Eibe and Mark (2011), a model with too many parameters relative to the number of training instances can become “too nonlinear”. It means that the model could perfectly fit a *training data* due to its many degrees of freedom and not because the model correctly represents the physical phenomena. Such a model performs very well on *training data* but poorly on *test data*. This phenomenon is known as overfitting, and can be minimized using structurally simpler models with fewer parameters (Witten; Eibe and Mark, 2011). As an attempt to reduce model complexity, a design of experiments was performed with the aim to investigate error response of the model for parameters change. The error was calculated by the root mean squared error (RMSE), between simulation and experimental data speeds, based on time step distribution. The relation of parameters values with model error is presented on Fig. 5.

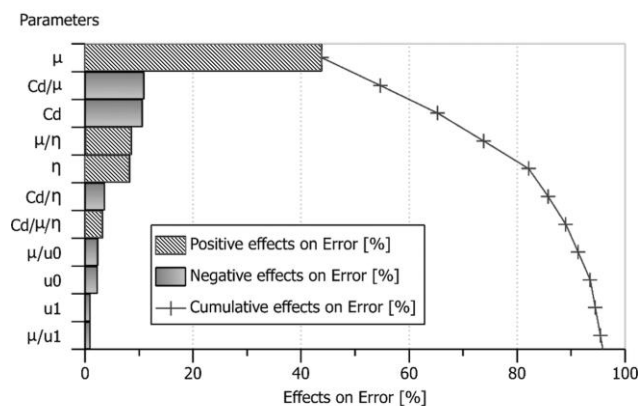


Figure 5: Pareto diagram of the effect of each model parameter on simulation error.

Negative effects means that if a parameter decreases, model error also decreases (e.g. if  $C_d$  is reduced, model error also reduces). Positive effect error means that if a parameter increases, model error also increases (e.g. if  $\mu$  rises, the model error rises too). The ratio between parameters, also included such as  $C_d/\mu$ ,  $\mu/\eta$  and  $C_d/\eta$ , effects model error in the same manner, model error increases if the ratio increases. From this diagram, some conclusions can be drawn. Friction coefficient ( $\mu$ ), driveline efficiency ( $\eta$ ) and drag coefficient ( $C_d$ ) account for more than 85% of effects on model error. Rolling resistance coefficients  $u_0$  and  $u_1$ , from Eq. (11), do not have significant influence on model error. Following the

recommendation of Witten, Eibe and Mark (2011) to avoid overfitting by using simpler models, rolling resistance coefficients were excluded from the parameter optimization process.

### 3.2 Monte Carlo parameter estimation

In order to understand the behavior of the model in response to input changes, several simulations were performed with the help of Monte Carlo method, a stochastic method that uses sampling random numbers to investigate a problem (SOLOMONEN, 2006). The reason to use this method was to cover a great number of parameters combinations to analyze its effects on model error. In this process, simulations of the vehicle speed profile were performed with different values of drag coefficient ( $C_d$ ), friction coefficient ( $\mu$ ) and driveline efficiency ( $\eta$ ).

The input parameters for these simulations came from pseudo-random values generated by an Optimized Latin Hypercube Sampling (OLHS) method with the help of AMESim® software. OLHS gives a uniform sampling and reduces the number of simulations needed in order to cover a high number of parameter combinations (Viana, 2013).

Each combination of parameters generated by the OLHS method was carried on to run the Monte Carlo simulations. Each simulation contained a set of random model input parameters predefined within a range according to typical values for similar racecars found on the literature.

Individual values for  $C_d$ ,  $\mu$  and  $\eta$  were collected as function of the sum of squared errors. However, when each isolated parameter is assigned based on its corresponding error, the error effect of other parameters are not being considered in the process. Therefore, there is a risk that specific combinations of parameters are potentially overfitting the model, which results in a misleading good performance of the simulation compared with *training data* that could fall short compared to *test data*.

To deal with this problem, the density of parameters values and its effects on model error were taken into account. Figure 6 are scatter plots of the simulations performed by the Monte Carlo optimization technique. The density of each scatter plot is given by the size of each grey circle. Then, to assign the estimated parameter, the key point was based on the minimum error given by the cloud boundary, represented in Fig. 6 by the dashed line, instead of individual values based on the smallest error found on the simulations.

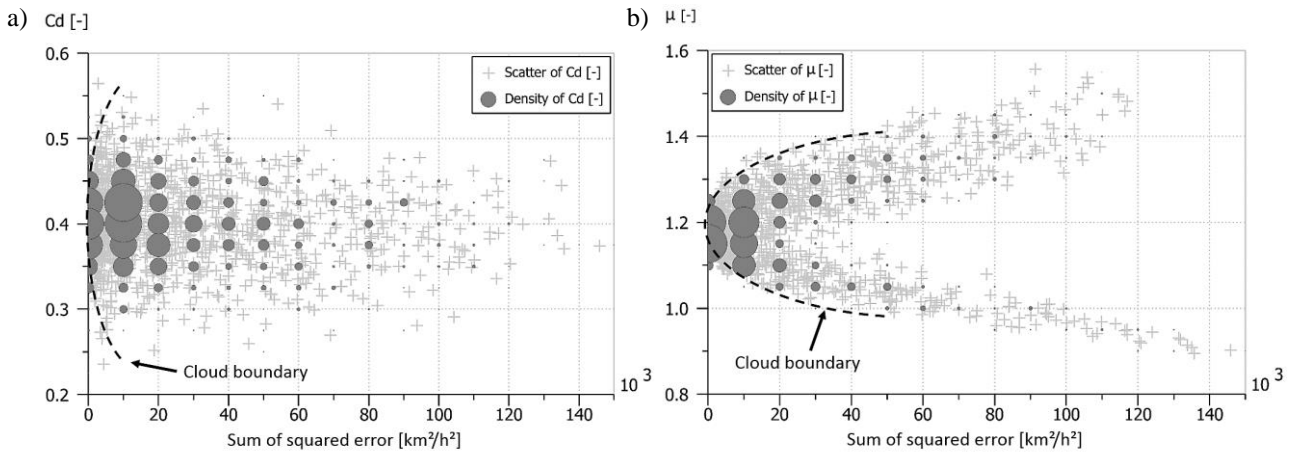


Figure 6: Density distribution of the sum of the squared error between Monte Carlo simulations and *training data*  $C_d$  (a) and  $\mu$  (b) shown.

In Fig. 6 (a), not surprising small errors occurs where the biggest density of drag coefficient  $C_d$  are close to the literature typical values of  $C_d \approx 0.40$  (Mcbeath, 2013, 2016). As this value diverges, model error increases. The sparse cloud of errors is assigned to random combinations of  $C_d$ ,  $\eta$  and  $u$ , which do not accurately represent the physical model.

Figure 6 (b) presents the effects of the coefficient of friction on simulation error. As expected, density distribution for small errors is concentrated in a smaller range of parameters (roughly,  $1.15 < \mu < 1.25$ ). The Pareto diagram (Fig. 5) already announced this characteristic, where the friction coefficient alone took more than 40% of effects on model error. In other words, this model is very sensible to changes in grip level of the circuit. This aspect can be a difficult issue to overcome while estimating a new circuit, since in the *test data* there is no chance to fine-tune grip level beforehand.

Applying the same technique to drivetrain efficiency, it was realized that  $\eta \approx 0.8$  produces smaller effects on model error. Table (1) summarizes the estimated parameter from the Monte Carlo optimization technique and the literature review.

Table 1: Summary of estimated parameters via Monte Carlo optimization and the literature review.

Parameter	Estimation Method		Literature reference
	Monte Carlo	Literature review	
$\eta$	0.80	0.72 – 0.91	(Irimescu; Mihon and Pădure, 2011)
$C_d$	0.40	0.30 – 0.44	(Mcbeath, 2013, 2016)
$u$	1.20	-	-

Accordinging Tab. (1), simulation error was decreased when values of drivetrain efficient ( $\eta$ ) and drag coefficient ( $C_d$ ) were set close to the average values found in the literature review.

## 4. SIMULATION RESULTS AND DISCUSSION

### 4.1 Ayrton Senna Circuit – GO, Brazil.

Figure 7 (a) indicates the position of some points of interest for the Ayrton Senna circuit map. The aim is to give a spatial reference for the discussion in the following paragraphs. In this figure, braking points and minimum speeds location are highlighted by tick marks along the circuit. At the right side, the upper plot of Fig. 7 (b) shows the simulated speed profile compared with *training data*, while the bottom part shows the residual values between them.

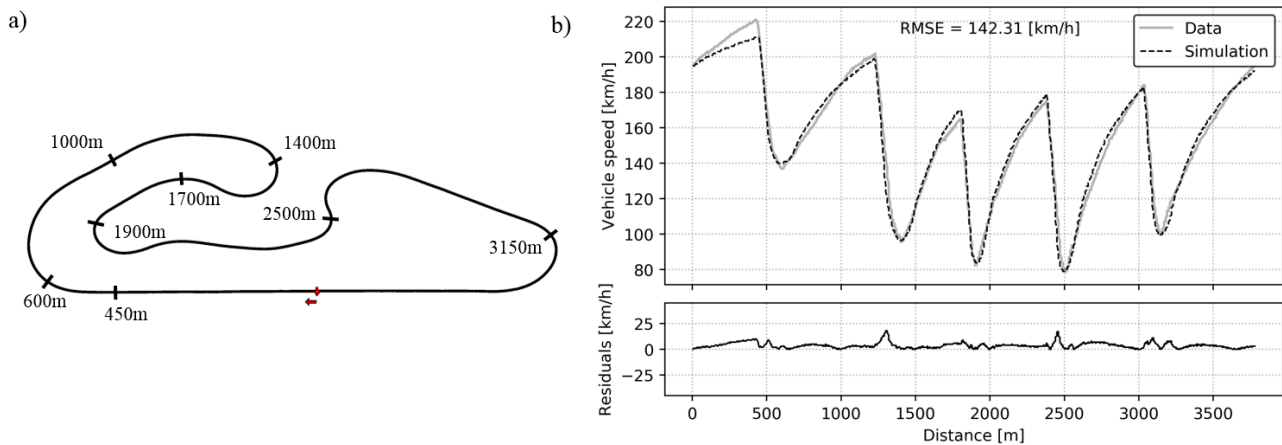


Figure 7: (a) reference points for the circuit map. (b) comparison between simulation and *training data*.

Simulation predicted a lap time of 93.30 seconds at Ayrton Senna Circuit, while the real fastest lap time was 93.14 seconds, 0.17% higher. The speed plot in Fig. 7 reveals differences between simulation and experimental data at the end of the main straight (< 450m). Predicted top speed was about 10 km/h lower than actual data due to higher external resistances presented in the model. At this location of the circuit (< 450m), speeds are above 200 km/h, which emphasizes lack of aerodynamic fit of the model. Furthermore, rolling resistance, also function of speed, may be acting in combination to over detract engine power. As stated in section 3.3, rolling resistance parameters were based on common values of passenger vehicles that may be inadequate for a racing tire. The evidence that for speeds below 180 km/h, this effect is less significant supports this hypothesis.

The vehicle model considers a constant friction coefficient between road and tire. For this reason, at some points it was expected to over or underestimate the grip available along the circuit. For instance, at the exit phase of corner 1 (> 600m), simulation overestimates the grip resulting in higher longitudinal acceleration than real data.

On the other hand, approaching the wide right hand turn at ~1000m, a crossover point between simulated and real speed trace is observed, i.e. simulation speed trace decreases and crosses the data trace. Two reasons are assigned: grip of the racetrack is underestimated, thus cornering speed is decreased; lack of aerodynamic and rolling resistance fit for speeds above 180km/h, also detracting cornering speed.

From ~1700m, simulation data in Fig 7 shows higher speeds than experimental data. At this location, the racecar is performing a left hand corner at wide-open throttle (WOT). The present vehicle model considers rolling resistance only in function of speed and consequently treats a WOT corner as a simple straight line. However, rolling resistance is also function of tire slip angle; higher slip angle produces higher rolling resistance forces (MILLIKEN; MILLIKEN, 1995). Therefore, simulation overestimates the acceleration capability of the racecar because it is not considering the additional rolling resistance from the tire slip angle.

Residual values, seen in Fig 7 (b), indicate differences right before the corner apexes, where speeds are minimum (600m, 1400m, 1900m, 2500m and 3150m). It happens because the accentuated inclination of the speed trace at the braking maneuvers makes the residuals between both speed traces much higher.

## 4.2 Cristais Circuit – MG, Brazil.

Figure 8 (a) provides reference points for the speed plot on Figure 8 (b). For the sake of simplicity, not all corners are discussed in this section. Reference points for the Cristais Circuit are composed by relevant low speed corner apexes (~80km/h).

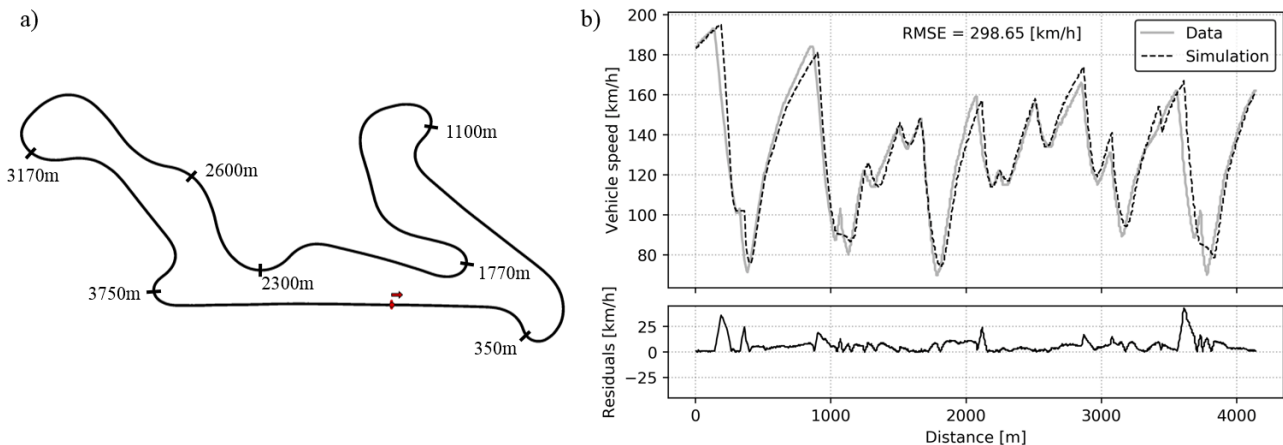


Figure 8: (a) reference points for the circuit map. (b) comparison between simulation and *test data*.

At Cristais Circuit, simulated lap was 121.20 seconds long and the real lap time took 124.30 seconds, a difference of 2.56%. Fig 8 (b) presents a comparison of simulated data with *test data* collected after the race event. Test data is a flying lap at the qualifying session at Cristais Circuit.

According to Fig. 8 (b), overall speed profile of the simulation follows the real speed trace of the logged data. The simulation captured main characteristics such as cornering speeds and braking points. Main differences between datasets were observed on braking maneuvers and at the apex of slow corners (around 80 km/h).

Alongside coefficient of friction, circuit parameterization was assigned as a source of errors, since it was designed solely with the driver's expertise of the racing line, not considering banks and differences at the grip level of the tarmac. According to the speed plot of Fig. 8 (~1000m and ~3700m), designed curvature profile was incapable to capture correctly details of tight cornering sequences.

Because the tire/road friction coefficient was estimated for the Ayrton Senna Circuit, differences were expected for the Cristais Circuit in comparison with *test data*. In fact, simulation overestimates the grip in almost all corners of Cristais Circuit (350 m, 1100 m, 1770 m, 3170 m and 3750 m) and its preceding braking points.

## 5. CONCLUSIONS AND FUTURE WORKS

In this work, a single-point mass vehicle model was presented with the aim to generate the speed profile of a new circuit. The model was developed in the multi-domain software AMESim®, which helped to speed up the process by skipping coding/debugging iterations to directly apply the physical model through object-oriented programming.

Unknown input parameters of the model were estimated using a Monte Carlo optimization process, where several simulations were run with different combinations of parameters. Each simulation was evaluated by a cost function of logged data from a known circuit. From these simulations, parameters estimations were based on their impact on simulation error. Finally, the simulation of the new circuit was performed and compared with the data collected after the race event. The parameters estimated were in accordance to the initial values taken from the literature. It suggests that for a simple model like a point-mass, typical values from the literature could be enough to simulate the speed profile of a racecar.

The results of the simulations helped the race engineers and drivers on the recognition of a new circuit. The baseline setup of the racecar was estimated through comparison of the speed profile of the new circuit to other known racetracks in the calendar. In conjunction with the driver's expertise, at the race event other characteristics of the circuit could be considered such as bumps, curbs and the racing line itself.

Future work includes nonlinear tire models and load transfer to further represent the interaction of vehicle setup with lap time simulation. Driver's technique and expertise should also be included, addressed by how G-G diagram is explored along the circuit.

## 6. ACKNOWLEDGMENTS

This paper was based upon a master thesis supported by CAPES (Coordination for the Improvement of Higher Education Personnel). The authors also would like to acknowledge RZ Motorsport racing team for their collaboration throughout this work.

## 7. REFERENCES

- Irimescu, A., Mihon, L., & Pădure, G., 2011. *Automotive transmission efficiency measurement using a chassis dynamometer*. International Journal of Automotive Technology.
- JAZAR, R.; N., 2008. *Vehicle Dynamics: Theory and Applications*. Springer US, Inc.
- Katz, J., 1995. *Racecar Aerodynamics*. Cambridge, MA: Bentley.
- Mcbeath, S. May 2013. *Tale of the tape*. Racecar Engineering. UK, v. 23, n. 5, p. 45-46.
- Mcbeath, S., Sep. 2016. *Subaru touring car aerodynamic study*. Racecar Engineering. UK, v. 26, n. 5, p. 57-58.
- Milliken, W. F.; Milliken, D. L., 1995. *Race car vehicle dynamics*. Warrendale, Society of Automotive Engineers.
- Rouelle, C., 2014. *Applied Vehicle Dynamics Seminar*. OptimumG, Denver, USA. 3-day seminar at Cologne University of Applied Sciences. Cologne, Germany. Nov 10-12.
- Segers, J., 2014. *Analysis techniques for racecar data acquisition*. Warrendale, PA: SAE International.
- Silva, J.C., 2005. *Virtual Environment for Dynamic Modelling of Multi-Domain Systems*. Proceedings of the 18th COBEM.
- Solonen, A. M., 2006. *Monte Carlo Methods in Parameter Estimation of Nonlinear Models*. Master's thesis, Lappeenranta University Of Technology.
- Viana, F. A. C., 2013. *Things you wanted to know about the Latin hypercube design and were afraid to ask*. 10th World Congress on Structural and Multidisciplinary Optimization, p. 1-9.
- Witten, I. H.; Eibe F. & Mark A. H., 2011. *Data Mining: Practical Machine Learning Tools and Techniques*.

## 8. RESPONSIBILITY NOTICE

The authors are the only responsible for the printed material included in this paper